Fractal Dislocation Patterning During Plastic Deformation

Peter Hähner,[1] Karlheinz Bay,[2] and Michael Zaiser[2]

[1]*European Commission, Joint Research Centre, I-21020 Ispra (Va), Italy*
[2]*Max-Planck-Institut für Metallforschung, Heisenbergstrasse 1, D-70569 Stuttgart, Germany*
(Received 13 May 1998)

During the later stages of plastic deformation, strain hardening of face-centered cubic metals goes along with the formation of cellular dislocation patterns appearing on various scales. The paper presents an analysis of the fractal geometry of these dislocation structures. A theoretical model is presented according to which dislocation cell formation is associated with a noise-induced structural transition far from equilibrium. The observed fractal dimensions are related to the stochastic process of dislocation glide, and implications for quantitative metallography are discussed. [S0031-9007(98)07147-6]

PACS numbers: 62.20.Fe, 05.40.+j, 61.72.Ff

The performance of solid materials is usually affected by the presence of defects: point defects, dislocations, cracks, and phase and grain boundaries. In some cases classical methods of materials characterization (e.g., in terms of mean particle size, average dislocation density, etc.) fail to describe properly defect microstructures which exhibit features of both randomness and heterogeneity. Owing to a high degree of disorder on various scales, stochastic methods are then needed to characterize and, possibly, predict and control the structural features. Fractal analysis then provides a tool to account for multiscale behavior and, hence, to address the important question of how the macroscopic properties of a material relate to its microscopic defect structure, e.g., the particle size distribution of dispersion strengthened materials or the arrangement of grains in multiphase materials [1]. In the present work, fractal analysis is applied for the first time to deformation-induced dislocation cell structures which are characterized by a hierarchy of mesoscopic scales (ranging from say 0.1 to 10 μm) [2]. The results are interpreted in terms of a stochastic dislocation dynamical model of cell formation.

The flow stress of metals deforming plastically by dislocation glide is governed by dislocation-dislocation interactions [3]. During deformation dislocations accumulate in the crystal which gives rise to work hardening. At the same time cellular dislocation patterns may develop spontaneously. These patterns consist of dislocation-rich "cell walls" separating dislocation-depleted cell interiors. Although the actual aspects of the cell structures depend on various extrinsic (e.g., strain rate, temperature, crystal orientation) and intrinsic (crystal structure, stacking fault energy, chemical composition) parameters, the propensity to dislocation patterning and its relation to work hardening are common to various materials.

Figure 1 shows a transmission electron micrograph of a cellular dislocation structure in a Cu single crystal deformed in tension. One notes the absence of a well-defined scale, as cells of various sizes appear. Obviously, the average cell size that is usually referred to in the metallurgical literature is not representative of this microstructural morphology. To verify the fractal nature of these structures,

Cu single crystals are considered after tensile deformation along a [100] axis, i.e., a symmetric multiple slip orientation leading to isotropic dislocation structures [5]. The crystals had been deformed at room temperature (strain rate 5×10^{-5} s^{-1}) to stresses (resolved shear stress in the active slip systems) $\tau^{\text{ext}} = 37.3$, 68.2, and 75.6 MPa, and micrographs taken from sections parallel and normal to the tensile axis [6]. In addition, comparable micrographs from the literature have been considered (Cu [100] deformed to $\tau^{\text{ext}} = 52$ [7], 67 [7], and 75.6 MPa [4]).

The micrographs were digitized to obtain binary maps of the cell walls ("black") and cell interiors ("white"). To estimate the fractal dimension, the box-counting method was applied: For grids of square boxes with edge length Δx, the number $N(\Delta x)$ of boxes containing at least one pixel of a cell wall is determined. A relation $N(\Delta x) \sim \Delta x^{-D_{\text{B}}}$ defines the "box-counting" dimension D_{B}. For the cell patterns investigated, double-logarithmic plots of $N(\Delta x) \times \Delta x^2$ vs Δx reveal three distinct regimes (see Fig. 2): (i) At very small Δx, $N \sim \Delta x^{-2}$, i.e., the slope of the plot becomes small. This is a consequence of the areal character of the cell walls which shows up at small scales. (ii) At intermediate Δx, linear scaling regimes
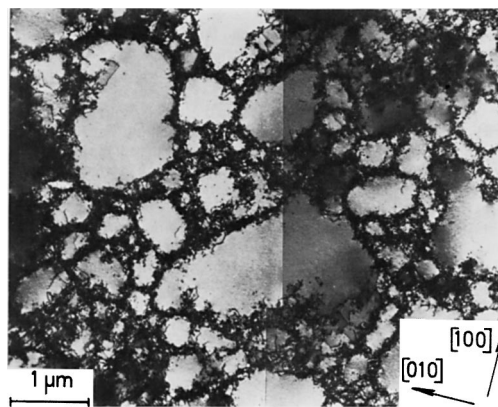

FIG. 1. Transmission electron micrograph of the dislocation cell structure of a Cu single crystal after tensile deformation along a [100] direction at room temperature to a stress of 75.6 MPa. After Mughrabi *et al.* [4].

0031-9007/98/81(12)/2470(4)$15.00

with fractional slope m are found to extend between 1 and 2 orders of magnitude. The corresponding box dimensions $D_B = 2 - m$ increase with stress, ranging from $D_B = 1.64 \pm 0.02$ at 37.3 MPa to 1.79 ± 0.01 at 75.6 MPa (cf. Fig. 4 below). (iii) At large Δx, N decreases again as Δx^{-2} after the largest cell within the analyzed area is covered completely. While scaling is bounded intrinsically from below due to the finite thickness of cell walls, the upper boundary is a finite size effect imposed by the sample area of the micrographs.

Complementary information is obtained from distributions of cell sizes λ. For a "hole fractal" [8] in two dimensions, a hyperbolic frequency distribution $N(\lambda > \Lambda) = C\Lambda^{-D_G}$ of cells with sizes greater than Λ defines the "gap dimension" D_G. The prefactor C which depends on cell shape, fractal dimension D_G, and the analyzed area A reads $C(D_G, A) = [4(2 - D_G)A/(\pi D_G)]^{D_G/2}$ for spherical cells [9]. Cell size distributions obtained from two different crystals are depicted in Fig. 3. Again, scaling over more than 1 order of magnitude is found. With the values $A = 32~\mu m^2$ for $\tau^{ext} = 75.6$ MPa and $A = 510~\mu m^2$ for $\tau^{est} = 68.2$ MPa, the gap dimensions D_G were determined by fitting curves $C(D_G)\Lambda^{-D_G}$ to the experimental data (solid lines in Fig. 3). This yielded $D_G = 1.78 \pm 0.04$ (75.6 MPa) and 1.85 ± 0.06 (68.2 MPa). Note that not only the hyperbolic behavior of the distributions, but also the A dependence of the scaling regime is reproduced correctly. This gives strong evidence that scaling is genuine and only delimited by finite size effects.

The fact that, within the limits of confidence, the values of D_G and D_B coincide (cf. Fig. 4), indicates that the roughness of the cell surfaces does not affect the fractal dimension and that the cell structures are indeed self-similar hole fractals. In this case, the fractal dimensions D of the cell arrangements in the three-dimensional (3D) crystals relate to the fractal dimensions $D_{G,B}$ determined from 2D electron micrographs, i.e., planar sections of the
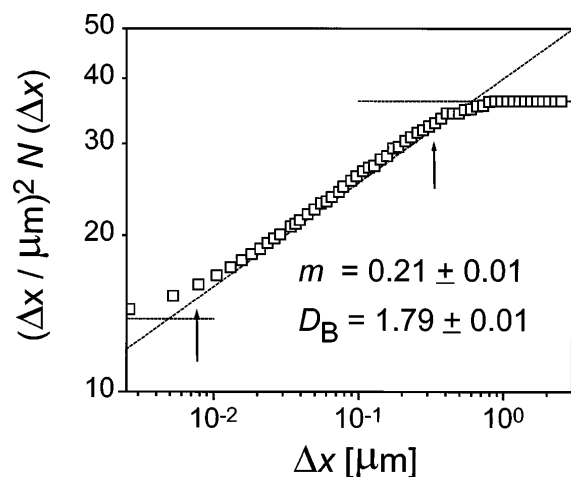
specimens, according to $D = D_{G,B} + 1$. These values have been compiled in Fig. 4.

To give a theoretical interpretation of our findings we consider collective dislocation glide as a stochastic process far from thermodynamic equilibrium [10,11]. As dislocations interact via long-range internal stresses (decaying as $1/r$ with distance r [12]), the mobile dislocations, i.e., the carriers of plastic strain, scan the stress fields produced by many other dislocations and thus experience appreciable fluctuations of the internal stress τ^{int} when gliding through the crystal. The effective stress, which is the difference of the external stress τ^{ext} (a smooth function in space and time) and the rapidly fluctuating internal stress, $\tau^{eff} = \tau^{ext} - \tau^{int}$, reflects those transient dislocation interactions. On the mesoscopic scale characteristic of dislocation patterning, this gives rise to spatiotemporal variations in the plastic shear strain rate $\dot{\gamma}$ produced by the mobile dislocation ensemble.

The fluctuation amplitudes of τ^{eff} and $\dot{\gamma}$ derive from requiring macroscopic stress equilibrium and using the Furutsu-Novikov theorem [13]. Formally, the results resemble fluctuation-dissipation theorems [10,11]:

$$\langle(\delta\tau^{eff})^2\rangle = S\langle\tau^{int}\rangle, \qquad \langle\delta\dot{\gamma}^2\rangle/\langle\dot{\gamma}\rangle^2 = \langle\tau^{int}\rangle/S. \quad (1)$$

The strain-rate sensitivity $S = \langle\dot{\gamma}\rangle(\partial\tau^{ext}/\partial\langle\dot{\gamma}\rangle)$ represents the *dynamic* response function to the average imposed strain rate $\langle\dot{\gamma}\rangle$. The correlation time t_{corr} of the fluctuations scales with the mean glide path L of the mobile dislocations (average density ρ_m) which is delimited by dislocation immobilization or annihilation: $t_{corr} = b\rho_m L/\langle\dot{\gamma}\rangle$, with the dislocation strength given by the modulus b of the Burgers vector.

The noisy character of dislocation glide is used in formulating a stochastic differential equation for the evolution of the total dislocation density ρ [11]. Since dislocations are line objects, it is not obvious how their density (total length per unit volume) evolves on a fractal topology
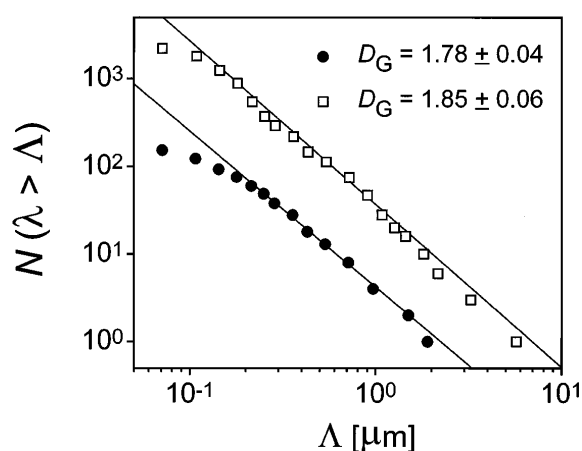

FIG. 2. Analysis of the cell structure in Fig. 1 by determining the "box dimension" D_B; for details see text.

$m = 0.21 \pm 0.01$
$D_B = 1.79 \pm 0.01$

FIG. 3. Cell size distributions in Cu single crystals deformed to stresses of 68.2 MPa (□) and 75.6 MPa (●) and determination of the respective gap dimensions D_G.

$D_G = 1.78 \pm 0.04$
$D_G = 1.85 \pm 0.06$

in 3D. Instead a 2D cross section of the crystal is considered where ρ represents the area density of dislocation intersection points with the plane and $1/\sqrt{\rho}$ gives their average distance in the plane. Accordingly, the following results relate directly to the situation observed on 2D micrographs. The dislocation balance involving generation and losses reads

$$\partial_t \rho = [\eta/E_L]\tau^{\text{ext}}\langle\dot{\gamma}\rangle - [\beta/b]\sqrt{\rho}\,[\langle\dot{\gamma}\rangle + \delta\dot{\gamma}]. \quad (2)$$

Here it is assumed that a fraction η of the mechanical work done per unit volume and time (i.e., $\tau^{\text{ext}}\langle\dot{\gamma}\rangle$) is stored in the form of elastic energy of dislocations, E_L is the dislocation line energy, and the parameter β gives the efficiency of dislocation density reduction due to dislocation reactions. Note that the mean free path for such reactions is proportional to the dislocation spacing $1/\sqrt{\rho}$ while $[\langle\dot{\gamma}\rangle + \delta\dot{\gamma}]/b$ is the (fluctuating) flux of moving dislocations. The strain rate fluctuations are approximated by a stationary Gaussian white noise with zero mean [14]: $\langle\dot{\gamma}(0)\dot{\gamma}(t)\rangle = 2\langle\delta\dot{\gamma}^2\rangle t_{\text{corr}}\delta(t)$. If we introduce dimensionless variables $\{\tilde{\rho}, \tilde{t}\}$ according to $\{\rho = [\eta b\tau^{\text{ext}}/(\beta E_L)]^2\tilde{\rho}, t = [\eta b^2\tau^{\text{ext}}/(\beta^2 E_L\langle\dot{\gamma}\rangle)]\tilde{t}\}$ and drop henceforth the tildes, Eq. (2) becomes

$$\partial_t \rho = 1 - \sqrt{\rho} - \sigma\sqrt{\rho}\,\delta w,$$

$$\sigma^2 = \frac{\beta^2 E_L}{\eta b^2 \tau^{\text{ext}}} \frac{\langle\tau^{\text{int}}\rangle}{S} b\rho_m L, \quad (3)$$

where δw represents a standard white process with $\langle\delta w(0)\delta w(t)\rangle = 2\delta(t)$.

Statistical information about dislocation patterning is obtained from the steady-state solution of the Fokker-Planck equation corresponding to Eq. (3). Using the Stratonovich calculus yields the probability distribution

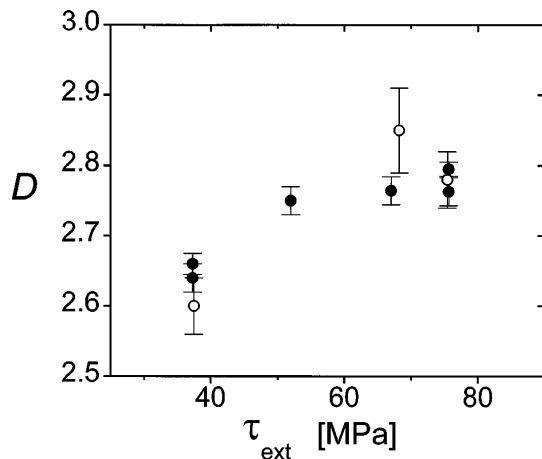$$p_s(\rho) = \mathcal{N}\rho^{-\alpha}\exp[-4\sqrt{\rho}/\sigma^2], \quad (4)$$

where $\alpha = (1/2)(1 - 4/\sigma^2)$ and $\mathcal{N}$ is a normalization constant. As the following discussion will show, this result (i) yields conditions which have to be met for dislocations to self-organize into cellular patterns and (ii) provides estimates of the fractal dimensions of the structures.

Figure 5 illustrates the qualitative changes occurring when the noise increases from small ($\sigma^2 \ll 1$) to large ($\sigma^2 > 4$) values. For small σ^2, the probability distributions possess maxima in the vicinity of the deterministic steady-state $\rho = 1$, while they fall off to zero both for $\rho \to 0$ and for $\rho \to \infty$. This situation corresponds to more or less homogeneous dislocation arrangements with well-defined mean density in space $\langle\rho\rangle$. The only characteristic length is the mean dislocation spacing $\langle\rho\rangle^{-1/2}$.

At the critical noise intensity $\sigma_c^2 = 4$ the maxima disappear giving way to monotonically decreasing probability distributions which, for $\sigma^2 > \sigma_c^2$, diverge as $\rho^{-\alpha}$ as ρ goes to zero. These hyperbolic distributions (with exponential cutoffs at a maximum dislocation density $\rho_{\max} = \sigma^4/16$) reflect the fact that dislocations organize on various scales down to an intrinsic minimum scale $\lambda_{\min} \sim 1/\sqrt{\rho}_{\max}$. The fractal dimension of the cell structures is obtained from noting that the mean dislocation spacing in a cell is proportional to the cell size, $\lambda \sim 1/\sqrt{\rho}$. Equation (4) is then transformed into a dislocation cell size distribution by change of variables $[p_s(\lambda)d\lambda = p_s(\rho)d\rho]$:

$$p_s(\lambda) \sim \lambda^{-\beta}\exp[-\lambda_{\min}/\lambda] \quad (5)$$

with $\beta = 3 - 2\alpha$. The corresponding cumulative cell size distributions function $P(\lambda > \Lambda)$ in 2D behaves as $P(\Lambda) \sim \Lambda^{-(2-2\alpha)}$. Hence the observed fractal dimensions can be related to the noise intensity. In 3D, one obtains $D = 2 + 4/\sigma^2$ which means that for those noise levels that give rise to hyperbolic probability distributions and dislocation cell patterning, $4 < \sigma^2 < \infty$, fractal dimensions range between the physically meaningful limits $3 > D > 2$. When $\sigma^2 > \sigma_c^2 = 4$ the dislocation structure ceases to fill up homogeneously the 3D specimens and
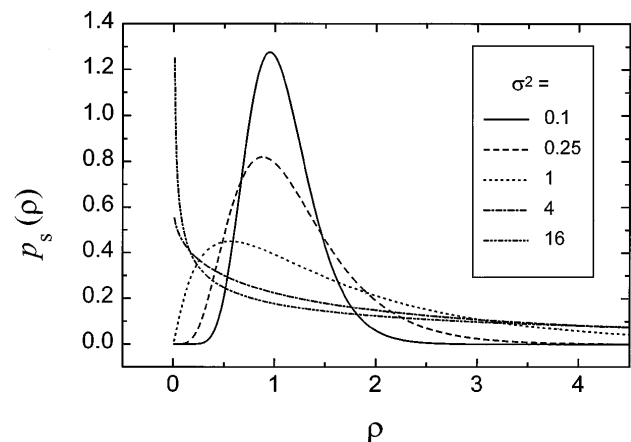
FIG. 4. Fractal dimensions D of dislocation cell structures of [100]-oriented Cu single crystals as a function of stress; filled symbols: $D = D_B + 1$ from box counting; open symbols: $D = D_G + 1$ from gap method.

FIG. 5. Steady-state probability distributions of the total dislocation densities for various values of the noise intensity σ^2.

spongy clustering sets in. This represents a noise-induced transition (control parameter σ^2) [15] from homogeneous dislocation arrangements to scale-invariant structures characterized by hyperbolic distributions of length scales.

A peculiarity of the system considered is that noise is generic to plastic flow by dislocation glide, since dislocations experience spatiotemporal stress fluctuations on the same range of mesoscopic scales where dislocation patterning takes place. Hence a stochastic description was chosen to reveal the information relevant to patterning. Being intrinsic the noise escapes direct external control. However, in view of the dependence of σ^2 on strain-rate sensitivity S [Eq. (3)] a wide range of noise levels can be realized for different materials and deformation conditions. In fact, bcc metals deformed at low temperatures possess considerably smaller ratios $\langle \tau^{\text{int}} \rangle / S$ than fcc metals. The correspondingly small noise σ^2 is in accordance with the rather homogeneous dislocation structures observed there [5]. The other extreme is found in dynamic strain aging alloys where interactions between moving dislocations and point defects may make S vanish ($\sigma^2 \rightarrow \infty, D = 2$). Accordingly, tuning deformation rate and/or temperature into this regime leads to a pronounced transition from homogeneous dislocation arrangements ($D = 3$) or cell structures ($3 > D > 2$) to planar dislocation arrays [16].

The observed stress dependence of the fractal dimension D (Fig. 4) can be related to the evolution of the various parameters affecting the noise σ^2, Eq. (3). As $\langle \tau^{\text{int}} \rangle / S$ shows only small variations with strain (Cottrell-Stokes law [3]), we focus on the evolution of the mobile dislocation density ρ_{m} and the mean glide path L with respect to stress τ^{ext}. When plastic flow proceeds without qualitative change in deformation mechanisms, $L \sim 1/\tau^{\text{ext}}$ holds. Then σ^2 is expected to decrease, as during strain hardening the mobile dislocation density increases at a rate smaller than $\sim (\tau^{\text{ext}})^2$. This explains why D is found to slightly increase with stress (Fig. 4).

To conclude we point out that deformation-induced dislocation cell structures are dominated by randomness rather than Euclidean order, and hence represent systems where "entropy wins over energy" [17]. This is to be contrasted with earlier attempts to interpret them as "low-energy dislocation structures" [18]. Moreover, the present analysis has shown that care must be taken when characterizing a cell structure in terms of an average cell size $\langle \lambda \rangle$. Since fractal behavior implies $\langle \lambda \rangle \sim \lambda_{\text{min}}$, the results of metallographic investigations depend sensitively on the transmission electron microscopy (TEM) magnification used. This gives a natural explanation for the large systematic and not as yet understood discrepancies regarding the average cell sizes reported by different authors [19].

[1] E. Hornbogen, Int. Mater. Rev. **34**, 277 (1989).

[2] In a paper by Gil Sevillano, Bouchaud, and Kubin [Scr. Metall. Mater. **25**, 355 (1991)] an attempt is reported to assess the fractal dimension D of cellular dislocation patterns by plotting the mean cell size $\langle \lambda \rangle$ determined from electron micrographs vs the TEM magnification M. Note that the minimum resolvable cell size $\lambda_{\text{min}}^{\text{res}} \sim 1/M$, while for a hyperbolic cell size distribution characterizing a fractal $\langle \lambda \rangle$ and $\lambda_{\text{min}}^{\text{res}}$ are proportional. Thus the procedure allows one to distinguish multiscale behavior ($\langle \lambda \rangle \sim M^{-1}$) from quasiperiodic structures ($\langle \lambda \rangle \approx \text{const}$), whereas a determination of D is not possible.

[3] J. Gill Sevillano, in *Materials Science and Technology*, edited by H. Mughrabi (VCH, Weinheim, 1993), Vol. 6, p. 19.

[4] H. Mughrabi, T. Ungar, W. Kienle, and M. Wilkens, Philos. Mag. A **53**, 793 (1986).

[5] Ch. Schwink, Scri. Metall. **27**, 963 (1992).

[6] We thank Dr. U. Essmann for providing these (unpublished) TEM micrographs.

[7] Y. Kawasaki and T. Takeuchi, Scr. Metall. **14**, 183 (1980); A. Goettler, Philos. Mag. **28**, 1057 (1973).

[8] P. Pfeifer and M. Obert, in *The Fractal Approach to Heterogeneous Chemistry*, edited by D. Avnir (Wiley, New York 1989), p. 11.

[9] This normalization is obtained by assuming that the scaling regime extends up to the cell size where the cumulative frequency distribution falls below 1.

[10] P. Hähner, Appl. Phys. A **62**, 473 (1996).

[11] P. Hähner, Acta Mater. **44**, 2345 (1996).

[12] F. R. N. Nabarro, Theory of Crystal Dislocations (Dover, New York, 1987), pp. 53ff.

[13] U. Frisch, *Turbulence: the Legacy of A. N. Kolmogorov* (Cambridge University Press, Cambridge, 1995), p. 43.

[14] The Gaussian white-noise approximation is justified by the fact that the correlation time t_{corr} is short as compared to the characteristic time of the systematic evolution of the dislocation density (which causes strain hardening). For the same reason we may concentrate without loss of generality on the steady-state probability density $p_s(\rho)$, Eq. (4). A more detailed analysis including the effects of a finite strain hardening rate will be presented elsewhere [M. Zaiser and P. Hähner (to be published)].

[15] W. Horsthemke and R. Lefever, *Noise-Induced Transitions* (Springer, Berlin, 1984).

[16] S. Flor and H. Neuhäuser (to be published).

[17] H. E. Stanley, in *Fractals and Disordered Systems*, edited by A. Bunde and S. Havlin (Springer, Berlin, 1991), p. 39.

[18] N. Hansen and D. Kuhlmann-Wilsdorf, Mater. Sci. Eng. **81**, 141 (1986).

[19] S. V. Raj and G. M. Pharr, Mater. Sci. Eng. **81**, 217 (1986).